Temperature Analysis of Single busbar With Variation of Total Harmonic Distortion in Current

Mohd Wafiuddin Yahya[1,2,*], Baharuddin Ismail[1,2], Afifah Shuhada Rosmi[1,2], Muhammad Mokhzaini Azizan[3], Mohamad Nur Khairul Hafizi Rohani[1,2], Chanuri Charin[1,2], Muhamad Hafiz Ab Aziz[2], Sharulnizam Mohd Mukhtar[1], Yazhar Yatim[1]

[1] Faculty of Electrical Engineering & Technology, Pauh Putra Campus, Universiti Malaysia Perlis, 02600 Arau, Perlis, Malaysia
[2] Centre of Excellent for Renewable Energy (CERE), Universiti Malaysia Perlis, Pauh Putra Campus, 02600 Arau, Perlis, Malaysia
[3] Department of Electrical and Electronic Engineering, Faculty of Engineering and Built Environment, Universiti Sains Islam Malaysia, 71800, Bandar Baru Nilai, Nilai, Negeri Sembilan, Malaysia

ARTICLE INFO	ABSTRACT
      	Typically, busbars are used to transmit and distribute currents in a bus duct system. The alarming use of nonlinear loads in the industrial sector or at residentials, such as arc welding, computers, ballast lighting, variable speed drives, and so on, has resulted in the generation of harmonics in current distortion, which are uncontrolled and thus increase heat generation within the system. The research conducted in this paper focuses on the prediction of the heat distribution as well as the analysis on operating temperature of a single busbar with compliance to the British National and International Standard (BS 159: 2014) using the Finite Element Method (FEM) in COMSOL Multiphysics software. The copper busbar dimension used for this research was 20mm x 6mm x 300mm, and the fundamental Root Mean Square (RMS) current was 419.1 A. The size of this busbars can withstand the maximum current of 430 A at a maximum operating temperature of 90°C, which complies with the standard requirement. The fundamental current is injected with variation of total harmonic distortion in current up to 55% with an interval of 5%. According to the findings, the operating temperature increases in direct proportion to the increase in total harmonic distortion with the current injections. With the presence of 55% of total harmonics in the current, the current was increased up to 57.73 A from the fundamental current, while the operating temperature was increased up to 14⁰C from the fundamental temperature. The total harmonics in current produced by the nonlinear loads could affect the operating temperature of the busbars, and this continuous operation of current flow will affect the busbars' lifespan due to the occurrence of overheating.

1. Introduction

Nowadays, busbar is a crucial component in power systems, communication base stations, military systems, transportation systems, energy, and other domains [1]. Generally, busbars are strips

---

* *Corresponding author.*
E-mail address: wafiuddin@unimap.edu.my

or bars commonly made of copper, brass, or aluminum that are used to transport electricity inside of switchboards, distribution boards, substations, battery banks, and other electrical equipment [2]. Many researchers around the world have studied and discussed busbar technology in terms of design, construction, and thermal analysis based on the applications' needs [3-13]. Research regarding busbar design and performance optimization was conducted by authors in [3], stated that the busbar, like other system components, must be able to withstand overheating pressures without being harmed. Basically, the materials for busbars should have excellent mechanical qualities and operate within a suitable temperature range. In Malaysia, copper and aluminum are the two typical materials used for busbars. Aside from density, copper is generally a better choice due to its capability and efficiency in transferring currents [4]. Furthermore, the busbar dimension should take temperature rise into account in order to permit ampacity and allow temperature rise with both natural and forced convection cooling arrangements. As a result, aluminum busbars haves a lesser current carrying capability than copper busbars.

The research analysis of temperature rises at the initial stage with an ambient temperature of $20^{o}C$ was conducted using FEM in order to ensure the structural integrity of the overall system with a variation of input phase current in order to define the temperature rise. As a result, due to fluctuations in the input phase current, the temperature rise fluctuated slightly [5-7]. Thus, according to the authors [8], FEM has been frequently employed up to this point for the bus duct system's temperature rise study. It has been demonstrated that the FEM produces excellent results when estimating the rise in temperature of the bus duct system. Another work that investigated the temperature rise was done by authors [9] in a different situation and focused on the effect of high current produced by power loads at switchgear in a distribution system. The accumulated data were analyzed in various ways and resulted in a few conclusions, including the significant pace of temperature increase. The regularity of the switchgear's temperature distribution is clearly impacted by the variable input current, ventilation equipment, and unbalanced current in a certain way. This situation creates overheating, which leads to power failure and consequently accidental explosion.

There have been few studies on the thermal consequences of power loss generation. According to the authors [10], a model was previously developed to examine the steady state and transient performance of a single busbar disregarding to the material or geometry, while in [11], a laminated bus bar was the subject of a scalable lumped parameter thermal model, with estimation and real temperatures being quite similar. In another method, a mathematical model relating to the distribution of a busbar's temperature rise from a high current power supply was described by the authors [12]. Depending on various electrical, geometrical, and mechanical criteria, thermal mathematical modelling can be used as a helpful tool to design various types of busbars with an adequate temperature distribution. It is also possible to obtain the results of a thermal simulation without purchasing expensive specialized software or PC hardware by using a straightforward mathematical calculation analysis. The authors [13] had done research about the thermal analysis of heat distribution in busbars during rated current flow. The rated current at the low voltage switchgear was determined using advanced coupled analyses such as Maxwell 3D, transient thermal, and fluent Computational Fluid Dynamics (CFD). The simulation results demonstrated that these simulations were a perfect tool for accurately modelling the architecture of low-voltage switchgear.

Voltage, current, or frequency abnormalities caused by power quality issues, especially harmonic distortion, can lead to the malfunction of delicate machinery or important devices [14-17]. Basically, harmonics were produced by the nonlinear loads, which caused distortions to the current drawn. Due to the presence of fundamental and harmonic components, the distorted current waveform generates various frequencies [18]. The growing use of power electronic devices in both the residential and industrial sectors is raising serious concerns on the harmonic distortion of power

distribution networks [19] and [20]. The common nonlinear loads typically include two types of power electronic front ends [21]. Diode-based rectifiers, which were used in electronic ballasts for Compact Fluorescent Lamps (CFLs) and Silicon Controlled Rectifier (SCR) like thyristor/triac were used in dimmers are some of the typical nonlinear loads [22]. Other devices such as televisions, computers, printers, Variable Speed Drives (VSD) and arc furnaces also contribute to the increase of harmonics. There are so many studies done by previous researchers on the harmonics effect either for residential or commercial sectors [23-29].

Current harmonics in busbars also have an impact on the forces that may cause busbar deflection, additional vibrations, or insulation break energies [30-31]. Additionally, a variety of harmonic frequencies contribute to the increase in busbar operating temperature, which can have an impact on all the components of the power distribution system. Due to the presence of harmonic current, this paper presents operating temperature investigations utilizing joule heating simulation in COMSOL Multiphysics and employs copper as the material. This investigation was examined in accordance with the British National and International Standard requirement (BS 159:2014) and the Austral Wright Metals table, which calls for a maximum temperature rise of 50°C in an environment with a maximum ambient temperature of 40°C [3], [32] and [33].

The section in the remainder of the article will be divided into the following sections. The technique will be covered in section 2 along with the computation process, simulation setup, and validation procedure. Section 3 will then discuss the outcomes of the simulations, and section 4 will wrap up the conclusions.

2. Methodology

This section discusses the steps taken in order to analyze the temperature rise of the busbars under nonlinear load operation. The general steps taken for the simulation process is shown in Figure 1. The first process is the measurement and calculation of the total harmonic current. The geometry, size, and material of the busbars were then determined and used as the primary reference points for the remaining process of the operation. The simulation work was conducted using the FEM in COMSOL Multiphysics. The end result of the temperature rise will be compared to the Austral Wright Metals Table and the BS 159:2014 standard for the validation process.

2.1 Defining the Total Harmonic Distortion of Current (THD$_i$) and Total RMS Current ($\sum I_{rms}$)

In order to define the power factor, Eq. (1) is used. Therefore, the value of the PF is 0.8. Then, the phase current was subsequently calculated using the Eq. (2).

$$pf = \frac{P}{S} \tag{1}$$

where, the power factor, pf, Real power (measured), P and the Apparent power (rated), S respectively.

$$I_{phase} = \frac{1000 \times P(kW)}{\sqrt{3} \times pf \times V_{LL}} \tag{2}$$

where, the power factor, pf, Real power (measured), P(kW) and Voltage, V_{LL} respectively.

The harmonic distortion is represented as total harmonic distortion of current (THD$_i$) in percentage units. THD$_i$ is determined by the proportion of harmonic currents to fundamental current, as shown in Eq. (3). A larger proportion denotes that the current contains more harmonic components which demonstrates that there is more distortion in the current. THD$_i$ was measured in the range of 15% to 40% according to measurement surveys that were conducted at a few locations [34], while for this research, the injected THD$_i$ is up to 55% in order to investigate the capability of the busbar with the selected sizing. Table 1 shows the rating at the measured location. From Eq. (2), the phase current supplied is 419.1 A.

Table 1
Rating at measured location

Phases	Frequency, f (Hz)	Apparent power, S (kVA)	Real power, P (kW)	Voltage, V_{LL} (V)
Three phases	50	300	241	415

This research applied the Fluke 1750 to extract and analyze the data on THD$_i$. The analysis comprises of the level of current harmonics at the point of common coupling in the power distribution system. By referring to the sizing table prepared by Austral Wright Metals, the dimension of a suitable busbar is 20mm x 6mm with a maximum current capacity of 430 A in free air operation, including a reduction of 1.5% error as the requirement for operation at 40°C ambient. The current rating valid for busbar in 40°C ambient temperature with a 50°C temperature rise operating condition corresponds to the British National and International Standards BS159:2014 [3] and [34].

$$THDi = \frac{\sqrt{\sum_{n=2}^{\infty} I_{n,rms}^2}}{I_1} \; x \; 100\% \tag{3}$$

Where, the fundamental RMS current, I_1 and the individual RMS current for the harmonic current, $I_{n,rms}$

Eq. (4) was used to determine the current value for the individual harmonic current or harmonic current amplitude from the harmonics order of 3rd, 5th, 7th, 9th and 11th.

$$I_{n,rms} = h_n\% \; x \; I_1 \tag{4}$$

Where, the individual RMS current for the harmonic current, $I_{n,rms}$, harmonic order (3rd to 11th) which represent as h_n and the fundamental RMS current, I_1. The results are tabulated in Table 3.

The total RMS current with the existing THD$_i$ for 5% to 55% can be calculated using the Eq. (5) where the results are tabulated in Table (4).

$$\sum I_{rms} = \sqrt{(I_1)^2 + (I_3)^2 + (I_5)^2 + (I_7)^2 + (I_9)^2 + (I_{11})^2} \tag{5}$$

2.2 Simulation Design and Setup

A flat rectangular copper busbar with a sectional area of 20mm × 6mm which can bear the maximum current of 430 A in free air operation was chosen as the dimension by referring based on

the table sizing of Austral Wright Metals. The length of the busbar was set at 300mm. The process for simulating the copper busbar design in COMSOL Multiphysics is outlined in the simulation flowchart in Figure 1.
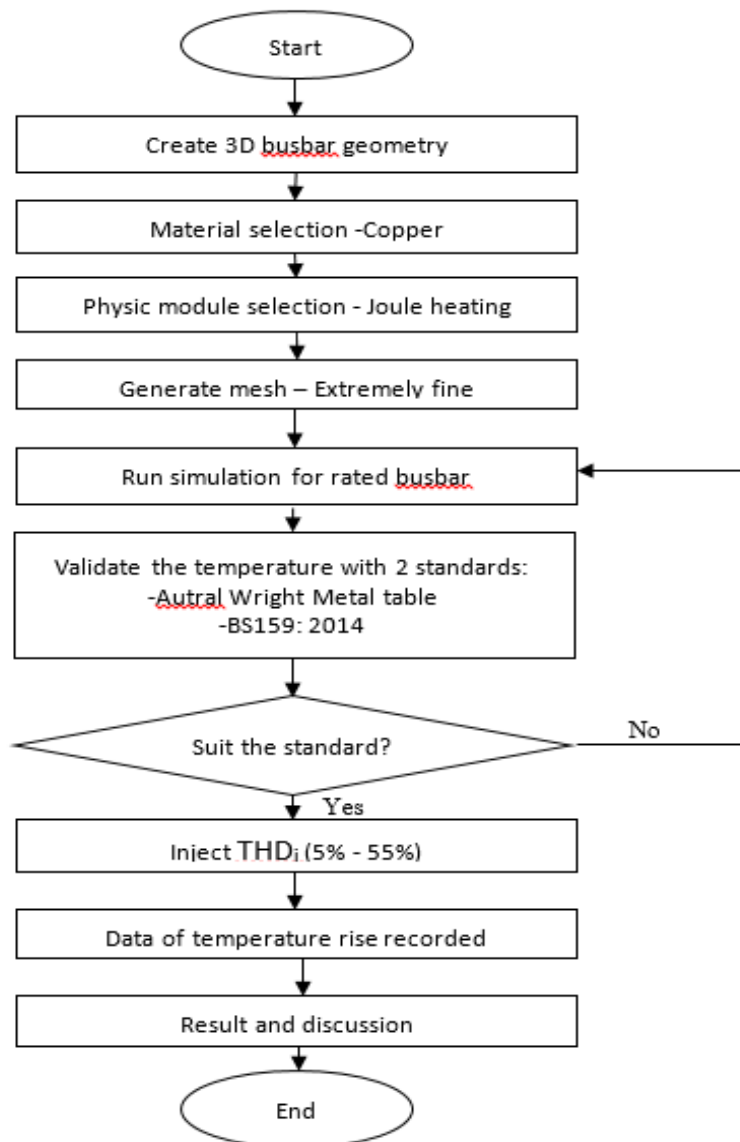

Fig. 1. Flowchart of Simulation Process in COMSOL Multiphysics

The simulations were carried out for both the linear and nonlinear condition. The first step is to declare global definitions. It served as the primary source of information for variables, functions, and parameters. Begin by developing 3D busbar geometry and then selecting materials for them in the design phase. The selection of physics modules is the next most critical step. This is the time to finish setting up the boundary conditions. Then, before moving on to the simulation study and computing the outcomes, it is a must to generate a mesh for geometry. The 3D design of the busbars with the chosen dimension are shown in Figure 2. The material selection for this research is copper and all the copper parameters are tabulate in Table 2.
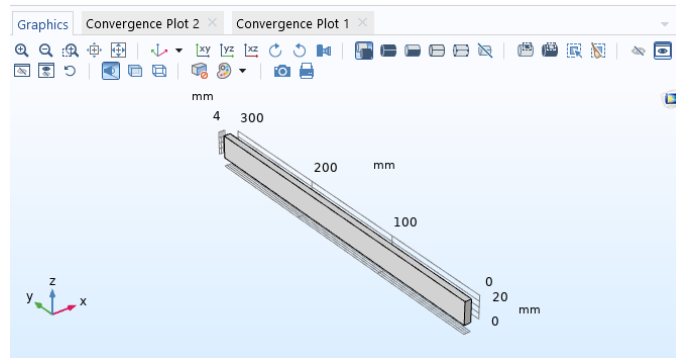
Fig. 2. 3D Design for the Dimension of 20mm x 6mm

The Joule heating effect, commonly known as the resistive heating effect, was defined by the electric current and energy conservation equation. Temperature and electric field are created by the two conservation laws, respectively. When an electric current flows through a material, the material heats up as a result of electric resistance. The thermal load was conceived of as a uniform volume heat source that was fed into the busbar power assembly as an input for the joule heating module. In order to analyze the thermal effect, the thermal simulation had been performed in this software, which is based on the FEM. It was set to extremely fine for the mesh generation, so the result will be more accurate.

Table 2
Parameters of Copper Busbar

Material	Conductivity (S/m)	Mass density (kg/m^3)	Heat capacity at constant pressure [J/(kg.K)]	Thermal conductivity [W/(m.K)]	Heat transfer coefficient for convection (W/m^{2}K)
Copper	5.81x10^7	8960	384	401	5 - 10

2.3 Validation Process

Simulations are only useful when the results match the behavior of the modelled system. This leads to problems with validation or verification, which let us make sure the outcomes are reliable and credible. In terms of the model's intended uses, validation is the process of determining if a simulation model and the data it uses accurately reflect the real world. The results of the simulation were evaluated using previous studies, a technical datasheet, and an international standard manual before moving on to further research and analysis. In this research, the current rating is valid for a single busbar on edge operating in a 40°C ambient temperature with a 50°C temperature rise, according to the Austral Wright Metals datasheet and the BS159:2014 standard. As for the validation process, the simulation result of temperature rise for the rated busbar will be compared to those datasheet and standard requirement.

3. Results

This work is assigned to analyse the temperature rise behaviour at the busbar itself according to the existing of THD$_i$ in the current fundamental. The result from the steps taken for this work will be discussed in this section.

3.1 THD$_i$ and $\sum I_{rms}$ Value

As for the harmonic current analysis, in order to identify the harmonic sequences, the nature of the 3rd, 5th, 7th and up to the nth harmonic orders can be assessed by using the fluke 1750, which can record data up until the 50th order of harmonic. This study considered harmonic current orders from 3rd to 11th only. The calculated individual RMS currents for the harmonic current based on the Eq. (3) and (4) are shown in Table 3.

Table 3
Calculation Result for I$_{n, rms}$ of 5% - 55% THD$_i$ of Each Harmonic Orders (3rd to 11th)

	HARMONIC ORDERS				
	3RD	5TH	7TH	9TH	11TH
5% THDi:					
Value (%)	4.13	2.22	1.14	0.93	0.73
In, rms (A)	17.13	9.31	4.75	3.88	3.05
10% THDi:					
Value (%)	7.71	3.14	2.83	2.34	2
In, rms (A)	32.13	13.2	11.9	9.88	8.4
15% THDi:					
Value (%)	11.2	5.87	4.61	4.29	3.98
In, rms (A)	46.8	24.6	19.3	18	16.7
20% THDi:					
Value (%)	14.7	8.86	6.04	5.09	4.61
In, rms (A)	61.6	37.12	25.32	21.34	19.3
25% THDi:					
Value (%)	18.42	11.06	7.47	7.29	6.8
In, rms (A)	77.19	46.35	31.3	30.54	28.51
30% THDi:					
Value (%)	22.4	13.34	8.9	8.81	6.61
In, rms (A)	93.87	55.89	37.3	36.94	27.72
35% THDi:					
Value (%)	25.86	15.94	10.79	10.36	7.2
In, rms (A)	108.36	66.81	45.21	43.4	30.17
40% THDi:					
Value (%)	30.15	17.87	13.4	10.65	8.3
In, rms (A)	126.37	74.91	56.12	44.62	34.79
45% THDi:					
Value (%)	34.6	19.83	14.19	11.25	8.93
In, rms (A)	144.98	83.11	59.49	47.16	37.41
50% THDi:					
Value (%)	38.06	21.99	16.1	12.78	10.05
In, rms (A)	159.53	92.17	67.35	53.57	42.14
55% THDi:					
Value (%)	41.35	24.38	17.8	14.15	11.1
In, rms (A)	173.33	102.19	74.51	59.32	46.53

As mentioned in Section 2.1, Eq. (5) was used in order to define the value of the total RMS current as tabulated in Table 4. Table 4 shows the calculation result for the fundamental RMS current and the total rms current with the harmonic current. When the fundamental RMS current was injected with the THD$_i$ from 5% to 55% with an interval of 5%, the value of the total RMS current increased, resulting in an increase in the operating temperature. From the result, the highest total RMS current

is 476.83 A, and this is clearly over the limit for the busbar size chosen, whereas the ampacity of the busbar is only 430 A. The increment was roughly around 57.73 A. The results also show that the rated dimension only has the capacity to withstand the total RMs current up to 20% of the THD_i, or 426.95 A. If the current is continuously flowing through the busbar with a higher RMS current, it surely cannot maintain its capacity, and the busbar will burn out due to the overheating. Therefore, a new size is required in order to maintain the busbar's capabilities.

Table 4
Calculated Result for The Total RMS Current (I_{rms})

THDi (%)	$\sum I_{rms}$ (A)
0	419.10
5	419.61
10	420.91
15	423.57
20	426.95
25	431.83
30	437.15
35	443.50
40	451.19
45	459.06
50	467.73
55	476.83

3.2 Temperature Analysis

Table 5 shows the simulation result of the temperature rise when THD_i of 5% to 55% were injected into the fundamental current. The results are illustrated in the graph of Figure 3. The temperature at 0% of THD_i is 87.720°C, as the fundamental or rated temperature. This value is considered valid for this experiment and suits the standard limits [3] and [26]. The operating temperature increased by about 14°C. Based on the result, the highest operating temperature was recorded as 101.72°C and this is clearly beyond the allowable limit for the busbar. The results also show that the rated dimension is only capable of withstanding the maximum total RMS current up to 20% of the THD_i, or 89.5°C. At 40% of THD_i which is the critical value, the temperature recorded was 95.2°C and this situation shows that the selected dimension of the busbar is no longer suitable to sustain the temperature. The highest THD_i injected to the busbar was recorded at a temperature of 101.720 °C. If the current is continuously flowing through the busbars, overheating will occur due to the higher existing of THDi, whereby the busbar will not be able to maintain its capacity to carry over load current thus causing malfunction or burn.

Table 5
Simulation Result for The Temperature Rise (°C)

THD_i (%)	Temperature (°C)
0	87.72
5	87.84
10	88.13
15	88.74
20	89.5
25	90.6
30	91.9
35	93.4

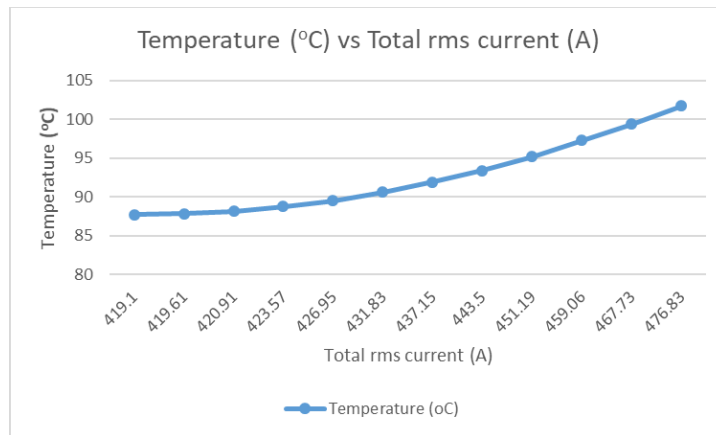| 40 | 95.2 |
45	97.3
50	99.4
55	101.72

Fig. 3. Temperature rise (℃) versus THD_i (%)

3.3 Temperature Distribution Image

Figure 4 represents the temperature of the maximum fundamental RMS current. The temperature recorded was 87.72℃. This result demonstrates that the rated temperature of the busbar is within the standard limits, which state that the allowance for temperature rise is 50℃ at an ambient of 40℃. As for the validation process, the selected dimension was suitable and followed the standard's limit requirements.
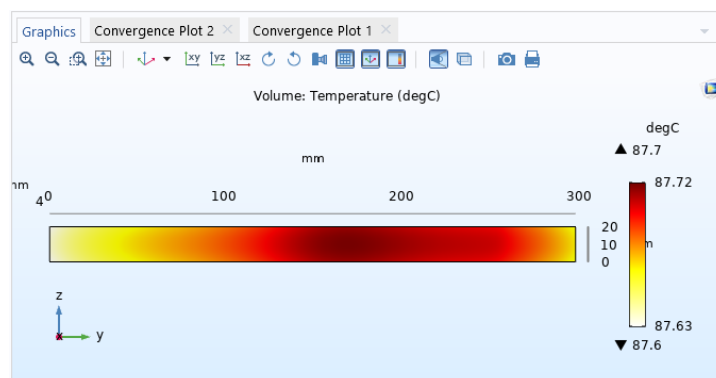

Fig. 4. Maximum Temperature at Fundamental Current

When the rated temperature was injected with the highest THD_i, which is 55%, the temperature was recorded at 101.72℃ and it was increased beyond the limits of what the busbar can carry where the results are shown in Figure 5. This situation is a very serious issue that should be taken into consideration during the selection of busbar size. The increasing of losses is due to the increased current flow through the busbar, which results in overheating. As a result, if the current continues to flow continuously for an extended period, the busbar cannot withstand the overheating and causing it to be malfunction or damaged.
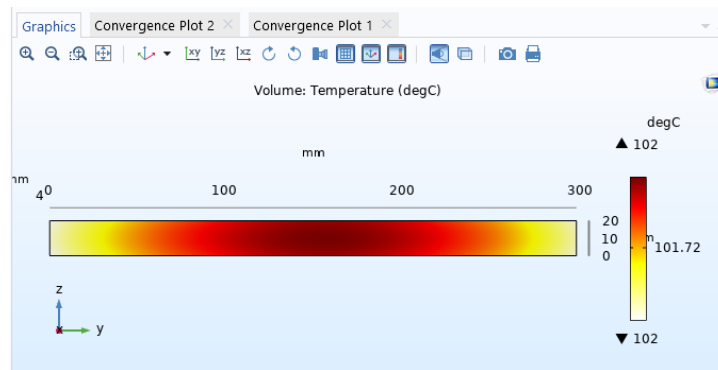
Fig. 5. Operating Temperature with Existing of 55% THDi

4. Conclusions

The temperature rise analysis of a single copper busbar has been successfully conducted using simulation in COMSOL Multiphysics software. It can be concluded that the temperature rise was successfully predicted and that it varied due to the amount of THD_i existing within the fundamental RMS current. The simulation results can be used to show the amount of temperature rise occurrences at steady-state current flow. This situation showing that harmonic in current also can be assume as a critical factor that can causing the temperature to rise and can harm the busbar's ability. The selection of busbar size is essential to ensure that the busbar can withstand the overcurrent due to the penetration of the THD_i and the tremendous usage of nonlinear load. This work can be referred to in the future as "knowledge direction" for designing a suitable busbars sizing and temperature rise prediction in order to fully satisfy the standard need.

References
[1] Bao, Y. J., Ka Wai Eric Cheng, K. Ding, and D. H. Wang. "The study on the busbar system and its fault analysis." In *2013 5th International Conference on Power Electronics Systems and Applications (PESA)*, pp. 1-7. IEEE, 2013. https://doi.org/10.1109/PESA.2013.6828246
[2] Shah, Prakruti, and Hetal Desai. "Overhead busbar design for 220/66 kv GIS substation." (2016).
[3] D. Chapman and T. Norris, "Copper for Busbars Guidance for Design and Installation," Copp. Dev. Assoc. Publ. No 22,pp.1–105,2014 [Online]. Available: http://copperalliance.org.uk/uploads/2018/03/copper_for_busbars_book_web_version.pdf.
[4] Thirumurugaveerakumar, S., M. Sakthivel, and Deve V. Sharmila. "Prediction and comparison of size of the copper and aluminium bus duct system based on ampacity and temperature variations using MATLAB." *Thermal Science* 22, no. 2 (2018): 1049-1057. https://doi.org/10.2298/TSCI160407153T
[5] Muhammood, Masri, Mohamad Kamrol, Dahaman Ishak, and Syafrudin Masri. "Temperature rise prediction in 3-phase busbar system at 20° C ambient temperature." In *2012 IEEE International Conference on Power and Energy (PECon)*, pp. 736-740. IEEE, 2012. https://doi.org/10.1109/PECon.2012.6450313
[6] W. A. Mustafa, N. M. Salleh, S. Z. S. Idrus, M. A. Jamlos, and M. N. K. H. Rohani, "Overview of Segmentation X-Ray Medical Images Using Image Processing Technique," J. Phys. Conf. Ser., vol. 1529, no. 4, pp. 0–9, 2020, doi: 10.1088/1742-6596/1529/4/042017.
[7] N. S. Othman et al., "An Overview on Overvoltage Phenomena in Power Systems," IOP Conf. Ser. Mater. Sci. Eng., vol. 557, no. 1, 2019, doi: 10.1088/1757-899X/557/1/012013.
[8] Ho, Siu Lau, Y. Li, X. Lin, H. C. Wong, and Ka Wai Eric Cheng. "A 3-D study of eddy current field and temperature rises in a compact bus duct system." *IEEE Transactions on Magnetics* 42, no. 4 (2006): 987-990. https://doi.org/10.1109/TMAG.2006.871632

[9] Xia, Haotian, Yonggang Guan, Zhanqing Yu, Suxiong Cai, Xiaorui Wang, Zhaowei Peng, Shisen Gao, and Zerong Huang. "Temperature rise test and analysis of high current switchgear in distribution system." *The Journal of Engineering* 2019, no. 16 (2019): 754-757. https://doi.org/10.1049/joe.2018.8371

[10] Coneybeer, Robert T., W. Z. Black, and R. A. Bush. "Steady-state and transient ampacity of bus bar." *IEEE Transactions on Power Delivery* 9, no. 4 (1994): 1822-1829. https://doi.org/10.1109/61.329515

[11] Smirnova, Liudmila, Raimo Juntunen, Kirill Murashko, Tatu Musikka, and Juha Pyrhönen. "Thermal analysis of the laminated busbar system of a multilevel converter." *IEEE Transactions on Power Electronics* 31, no. 2 (2015): 1479-1488. https://doi.org/10.1109/TPEL.2015.2420593

[12] Plesca, Adrian. "Thermal analysis of busbars from a high current power supply system." *Energies* 12, no. 12 (2019): 2288. https://doi.org/10.3390/en12122288

[13] Szulborski, Michał, Sebastian Łapczyński, and Łukasz Kolimas. "Thermal analysis of heat distribution in busbars during rated current flow in low-voltage industrial switchgear." *Energies* 14, no. 9 (2021): 2427. https://doi.org/10.3390/en14092427

[14] Kalair, A., Naeem Abas, A. Raza Kalair, Zahid Saleem, and Nasrullah Khan. "Review of harmonic analysis, modeling and mitigation techniques." *Renewable and Sustainable Energy Reviews* 78 (2017): 1152-1187. https://doi.org/10.1016/j.rser.2017.04.121

[15] C. C. Yii, M. N. K. H. Rohani, M. Isa, S. I. S. Hassan, B. Ismail, and N. Hussin, "Multi-end partial discharge location algorithm based on trimmed mean data filtering technique for MV underground cable," 2015 IEEE Student Conf. Res. Dev. SCOReD 2015, pp. 345–350, 2015, doi: 10.1109/SCORED.2015.7449353.

[16] S. H. K. Hamadi et al., "Modelling of partial discharge signal and noise interference using labview," IEEE Student Conf. Res. Dev. Inspiring Technol. Humanit. SCOReD 2017 - Proc., vol. 2018-January, pp. 451–455, 2017, doi: 10.1109/SCORED.2017.8305441.

[17] S. Xin Ni, O. Siew Har, and H. Li Vern, "Semarak International Journal of Machine Learning Dimensions Affecting Consumer Acceptance towards Artificial Intelligence (AI) Service in the Food and Beverage Industry in Klang Valley," Semarak Int. J. Mach. Learn., vol. 1, no. 1, pp. 20–30, 2024.

[18] Kütt, Lauri, Eero Saarijärvi, Matti Lehtonen, Heigo Molder, and Toomas Vinnal. "Harmonic load of residential distribution network—Case study monitoring results." In *2014 Electric Power Quality and Supply Reliability Conference (PQ)*, pp. 93-98. IEEE, 2014. https://doi.org/10.1109/PQ.2014.6866791

[19] Farrag, Mohamed Emad, Ayman Haggag, Haroon Farooq, and Waqas Ali. "Analysis and mitigation of harmonics caused by air conditioners in a distribution system." In *2017 Nineteenth International Middle East Power Systems Conference (MEPCON)*, pp. 702-707. IEEE, 2017. https://doi.org/10.1109/MEPCON.2017.8301258

[20] N. Mawar Hanifah Nik Hassan et al., "Unveiling Collaborative Trends in Fuzzy Delphi Method (FDM) Research: A Co-Authorship Bibliometrics Study," Int. J. Adv. Res. Comput. Think. Data Sci. J. homepage, vol. 2, no. 1, pp. 1–20, 2024, [Online]. Available: https://semarakilmu.com.my/journals/index.php/ctds/index.

[21] McBee, Kerry D., and Marcelo G. Simões. "Evaluating the long-term impact of a continuously increasing harmonic demand on feeder-level voltage distortion." *IEEE Transactions on Industry Applications* 50, no. 3 (2013): 2142-2149. https://doi.org/10.1109/TIA.2013.2288606

[22] Dghim, Hedi, Ahmed El-Naggar, and Istvan Erlich. "Harmonic distortion in low voltage grid with grid-connected photovoltaic." In *2018 18th international conference on harmonics and quality of power (ICHQP)*, pp. 1-6. IEEE, 2018. https://doi.org/10.1109/ICHQP.2018.8378851

[23] Bajagain, Surendra, and Anamika Dubey. "Harmonic Distortion Analysis in North American Residential Power Distribution Systems." In *2021 IEEE Power & Energy Society General Meeting (PESGM)*, pp. 1-5. IEEE, 2021. https://doi.org/10.1109/PESGM46819.2021.9637989

[24] Anu, G., and Francis M. Fernandez. "Identification of harmonic injection and distortion power at customer location." In *2020 19th international conference on harmonics and quality of power (ICHQP)*, pp. 1-5. IEEE, 2020. https://doi.org/10.1109/ICHQP46026.2020.9177869

[25] Roslizan, N. D., M. N. K. H. Rohani, C. L. Wooi, M. Isa, B. Ismail, A. S. Rosmi, and W. A. Mustafa. "A review: Partial discharge detection using UHF sensor on high voltage equipment." In *Journal of Physics: Conference Series*, vol. 1432, no. 1, p. 012003. IOP Publishing, 2020. https://doi.org/10.1088/1742-6596/1432/1/012003

[26] Niitsoo, J., I. Palu, J. Kilter, P. Taklaja, and T. Vaimann. "Residential load harmonics in distribution grid." In *2013 3rd International conference on electric power and energy conversion systems*, pp. 1-6. IEEE, 2013. https://doi.org/10.1109/EPECS.2013.6713054

[27] Michalec, Łukasz, Michał Jasiński, Tomasz Sikorski, Zbigniew Leonowicz, Łukasz Jasiński, and Vishnu Suresh. "Impact of harmonic currents of nonlinear loads on power quality of a low voltage network–review and case study." *Energies* 14, no. 12 (2021): 3665. https://doi.org/10.3390/en14123665

[28] Nanyan, Ayob Nazmy, Muzamir Isa, Haziah Abdul Hamid, Mohamad Nur Khairul Hafizi Rohani, and Baharuddin Ismail. "The rogowski coil sensor in high current application: A review." In *IOP Conference Series: Materials Science*

and Engineering, vol. 318, no. 1, p. 012054. IOP Publishing, 2018. https://doi.org/10.1088/1757-899X/318/1/012054

[29] Puchalapalli, Sambasivaiah, and Naran M. Pindoriya. "Harmonics assessment for modern domestic and commercial loads: A survey." In *2016 International Conference on Emerging Trends in Electrical Electronics & Sustainable Energy Systems (ICETEESES)*, pp. 120-122. IEEE, 2016. https://doi.org/10.1109/ICETEESES.2016.7581371

[30] Lepretre, P., M. Mary, and J. Schonek. "Taking account of harmonic currents in the selection of-busbar systems." In *2004 11th International Conference on Harmonics and Quality of Power (IEEE Cat. No. 04EX951)*, pp. 41-45. IEEE, 2004. https://doi.org/10.1109/ichqp.2004.1409326

[31] S. A. Roslan et al., "The Novel Method in Validating the Spectral Wavelength Optimization to Determine Archaeological Proxies by the Integration of Aerial and Ground Platforms," *J. Adv. Res. Appl. Mech.*, vol. 108, no. 1, pp. 1–15, 2023, doi: 10.37934/aram.108.1.115.

[32] Nabil, Mohammed, Mohamed Helmy Megahed, and Mohamed Hassan Abdel Azeem. "Design and simulation of new one time pad (OTP) stream cipher encryption algorithm." *Journal of Advanced Research in Computing and Applications* 10, no. 1 (2018): 16-23.

[33] Radzi, MZ Mohd, M. M. Azizan, and B. Ismail. "Observatory case study on total harmonic distortion in current at laboratory and office building." In *Journal of Physics: Conference Series*, vol. 1432, no. 1, p. 012008. IOP Publishing, 2020. https://doi.org/10.1088/1742-6596/1432/1/012008

[34] Nasini, Purushothama Rao, Narender Reddy Narra, and A. Santosh. "Modeling and harmonic analysis of domestic/industrial loads." *International Journal of Engineering Research and Application (IJERA)* 2, no. 5 (2012): 485-491.